SUPPLEMENTARY INFORMATION

Supplementary information includes supplementary experimental procedures and seven figures (Figure S1-S7).

Supplementary Experimental Procedures

Antibodies. Anti-mouse Runx2 (8486), Notch1 (4380), Notch2 (5732), Jag1 (2620), NICD (2421), Dnmt1 (5032), and Dnmt3a (2160) antibodies were purchased from Cell Signaling Technology (Danvers, MA, USA). Anti-GFP (A-11122) and rabbit IgG-Alexa Fluor 488 antibodies (A-11034) were purchased from Invitrogen (Carlsbad, CA, USA). Anti-mouse Fas (sc-1023), ALP (sc-28904), CD63 (sc-15363), CD81 (sc-9158), Rab27a (sc-22756) and Dnmt3b (sc-10236) antibodies were purchased from Santa Cruz Biotechnology (Santa Cruz, CA, USA). Anti-mouse CD3 (100208) and CD28 (102112) antibodies were purchased form BioLegend (San Diego, CA, USA). Anti-mouse CD3 (ab16669) antibody was purchased from Abcam (Cambridge, MA, USA). Anti-β-actin antibody (A1978) was purchased from Sigma (St. Louis, MO, USA). Anti-mouse CD73-PE antibody (550741) was purchased from BD Biosciences (San Jose, CA, USA). Anti-rat IgG-PE antibody (3030-09) was purchased from Southern Biotech (Birmingham, AL, USA). Anti-Fas ligand (FasL) antibody (16-5911) was purchased from eBioscience (San Diego, CA, USA).

Western blot analysis. Total protein was extracted using M-PER mammalian protein extraction reagent (Thermo, Rockford, IL, USA). Protein was applied and separated on 4–12% NuPAGE gel (Invitrogen) and transferred to Immobilon^{TM}-P membranes (Millipore, Bedford, MA, USA). The membranes were blocked with 5% non–fat dry milk and 0.1% tween–20 for 1 hour, followed by incubation with the primary antibodies (1:200–1,000 dilution) at 4°C overnight. Horseradish peroxidase–conjugated IgG (Santa Cruz Biosciences; 1:10,000) was used to treat the membranes for 1 hour, after which the membranes were enhanced with a SuperSignal West Pico

Chemiluminescent Substrate (Thermo). The bands were detected on films (Bioland, Paramount, CA, USA). β-actin antibody was used to quantify the amount of loaded protein.

Micro-CT and analysis. After being harvested and fixed in 4% paraformaldehyde (PFA), femurs were analyzed by high resolution Scanco μCT50 scanner (Scanco Medical AG, Bruttisellen, Switzerland). The specimens were scanned using a voxel size of 20 μm at 70kVp and 200 μA. Scanned data was reconstructed using Scanco software. Datasets were loaded into Amira 5.3.1 software (Visage Imaging, Berlin, Germany) for visualization and analysis. Bone mineral density (BMD) and bone volume/total volume (BV/TV) for each specimen were also calculated by using Amira software.

Bone histomorphometric analysis. For double calcein labeling, calcein green (Sigma, 10 mg/kg body weight) was intraperitoneally injected into mice at 7 days and 2 days before euthanasia. The fourth lumbar vertebrae were dehydrated and embedded without decalcification into methyl methacrylate (MMA) for sectioning with a Leica SM2500 microtome (Leica Microsystems, Germany). Bone dynamic histomorphometric analyses for MAR and BFR/BS were performed using Image J image analysis software under fluorescence microscopy (Olympus IX71, Japan).

MicroRNA mimic and inhibitor transfection. For *in vitro* studies, the miR-29b mimics, inhibitors and negative controls (Qiagen) were transfected into cells according to the manufacturer's instructions. For *in vivo* studies, Invivofectamine 2.0 (Invitrogen) and miR-29b inhibitors (*mir*Vana™ miRNA Inhibitors, Life Technologies, Carlsbad, CA, USA) were intravenously infused into MRL/*lpr* mice (7 mg/kg of body weight) at 10 weeks of age according to the manufacturer's instructions. The negative controls (*mir*Vana™ miRNA Inhibitors, Life

Technologies) of the inhibitors were used in control groups. The treatments were performed once a week for 4 weeks. For further analysis, the mice were sacrificed four weeks after the first treatment (a total of 4 treatments).

Methylation-specific PCR and bisulfite sequencing. Bisulfite conversion was performed using the EZ DNA Methylation-Gold^{TM} Kit (Zymo Research, Irvine, CA, USA) according to the manufacturer's instructions. For methylation-specific PCR, bisulfite-modified DNA was amplified with methylation-specific primers for Notch1 and Jag1, designed by MethPrimer (http://www.urogene.org/methprimer/). The primers for Notch1 (-1053 to -834) were: forward, 5'-TTAGGGATTAGTGAGAAGGGTGAT-3' and reverse, 5'- CATCAAAAAAATTAAAAC CAAACACT-3'; for Notch1 (-378 to -253): forward, 5'- TAGGGTTTATAAGGGG GTAAGG-3' and reverse, 5'- CAAAAACACTAATAAAACTCTAAAC-3'; for Notch1 (+931 to +1193): forward, 5'- GGAATTTTTTTTAAGTGGGGTTTT-3' and reverse, 5'- AAAAAATAACCACACTCAACTCCC-3'. Amplified PCR products were gel-purified with the QIAquick Gel Extraction Kit (Qiagen) according to the manufacturer's instructions. The cDNA was then cloned into pCR-TOPO vectors (Invitrogen) and transformed in competent E. coli (Invitrogen) for sequencing. Ten colonies were randomly chosen for sequencing (Genewiz, La Jolla, CA, USA).

siRNA knockdown. siRNAs for Dnmt1, Dnmt3a, Dnmt3b, Rab27a and Fas were used to treat the BMMSCs according to the manufacturer's instructions (Santa Cruz Biotechnology). Non-targeting control siRNAs (Santa Cruz Biotechnology) were used as negative controls. For *in vivo* siRNA knockdown studies, Invivofectamine 2.0 (Invitrogen) and Notch1 siRNA (Ambion

In Vivo siRNA, Life Technologies) were intravenously infused into MRL/*lpr* mice (7 mg/kg of body weight) at 10 weeks of age according to the manufacturer's instructions. The negative control siRNA (Ambion *In Vivo* siRNA, Life Technologies) was used in control groups. The treatments were performed once a week for 4 weeks. For further analysis, the mice were sacrificed 4 weeks after the first treatment (a total of 4 treatments).

Real-time polymerase chain reaction (PCR) of mRNA and miRNA. Total RNA was isolated from the cultures using the miRNeasy Mini Kit (Qiagen) according to the manufacturer's instructions. Total RNA from culture medium, serum and bone marrow supernatant was isolated using miRNeasy Serum/Plasma Kit (Qiagen). For real-time PCR of mRNA, the cDNA was synthesized using SuperScript III (Life Technologies). The real-time PCR was performed using SYBR green supermix (Bio-Rad, Hercules, CA, USA) and gene-specific primers. The primers included Dnmt1: forward, 5'-TGGTGAAGTTTGGTGGCACT-3' and reverse, 5'-TCACCG CCAAGTTAGGACAC-3'; GAPDH: forward, 5′-CACCATGGAGAAGGCCGGGG-3′ and reverse, 5′-GACGGACACATTGGGGGTAG-3′. For real-time PCR of mature miRNA, cDNA was synthesized using the miScript II RT Kit (Qiagen). Real-time PCR was performed using the miScript SYBR Green PCR Kit (Qiagen). RUN6 was used as an endogenous control for BMMSCs. MiR-39 was used a spike-in control for culture medium, serum and bone marrow (Qiagen). For real-time PCR of pri-miRNA, cDNA was synthesized using the High Capacity RNA-to-cDNA Kit (Life Technologies). Real-time PCR was performed using the TaqMan® Gene Expression Master Mix (Life Technologies) and primers specific for pri-miR-29b and GAPDH (endogenous control) (Life Technologies). Real-time PCR was detected on a CFX96™

Real-Time PCR System (Bio-Rad).

Plasmids. For overexpression, Dnmt1 expression plasmids (InvivoGen, San Diego, CA, USA) and Fas expression plasmids generated in our previous study (Akiyama et al., 2012) were used. EGFP expression plasmids (Addgene) were used as a control. For protein tracing, FAS-EGFP fusion protein expression plasmids (System Biosciences, Mountain View, CA, USA) were used. The empty plasmids with the same backbone were used as a control. The cells were transfected with plasmids using Lipofectamine LTX with Plus reagent (Life Technologies) according to the manufacturer's instruction.

Flow cytometry analysis. MRL/*lpr* BMMSCs were treated with exosomes (20 μg/ml) derived from BMMSCs transfected with plasmid containing Fas-EGFP fusion protein as described above. For detection of Fas-EGFP fusion protein *in vivo*, colonies were prepared as described above. Cells were incubated with 1 μg of CD73-PE antibody for 30 minutes on ice. Samples were analyzed using a fluorescence-activated cell sorting (FACS)^{Calibur} flow cytometer (BD Bioscience). At 24 hours after MSCT or exosome infusion (100 μg) into MRL/*lpr* mice, the apoptotic cells in lymph nodes were detected by staining with CD3 antibody, followed by AnnexinV Apoptosis Detection Kit I (BD Bioscience) and then analyzed by (FACS)^{Calibur} flow cytometer. For cell sorting, CD73 positive cells were sorted from bone marrow cells using CD73-PE antibody and a BD FACS Aria II Flow Cytometer (BD Bioscience).

Cell survival and apoptosis assay. C3H/HeJ or MRL/*lpr* BMMSCs (0.2×10^6/well) were seeded in 24-well plates (Corning). MRL/*lpr* BMMSCs were pretreated with exosomes (20 μg/ml) derived from C3H/HeJ BMMSCs, MRL/*lpr* BMMSCs or MRL/*lpr* BMMSCs transfected

with Fas expression plasmids for 24 hours. Activated spleen cells (1×10^6/well), which were pre-stimulated with plate-bound anti CD3 antibody (3 μg/ml) and soluble anti CD28 antibody (2 μg/ml) for 2 days, were loaded directly on BMMSCs. The cells were co-cultured in the absence or presence of anti-FasL antibody (1 μg/ml) in Dulbecco's Modified Eagle Medium (DMEM, Lonza, CH-4002 Basel, Switzerland) supplemented with 10% heat-inactivated FBS, 50 μM 2-mercaptoethanol, 10 mM HEPES (Sigma), 1 mM sodium pyruvate (Sigma), 1% non-essential amino acid (Cambrex, East Rutherford, NJ, USA), 2 mM L-glutamine, 100 U/ml penicillin and 100μg/ml streptomycin. After two days of co-culture, the wells were washed with PBS and stained using a fixing/staining solution containing 2% PFA and 2% toluidine blue. For detection of BMMSC apoptosis, after 12 hours of co-culture, the cells were stained with a terminal deoxynucleotidyl transferase dUTP nick end labeling (TUNEL) kit (In Situ Cell Death Detection Kit; Roche, Mannheim, Germany) according to the manufacturer's instructions. At 24 hours after MSCT or exosome infusion (100 μg) into MRL/*lpr* mice, the single suspension of cells in lymph nodes was used for TUNEL staining combined with immunofluorescence using antibodies against CD3.

Co-culture of C3H/HeJ BMMSCs and MRL/*lpr* BMMSCs. The transwell system for 6-well plates (Corning) was used for co-culture experiments. MRL/*lpr* BMMSCs (0.3×10^6) were loaded in each lower chamber. C3H/HeJ BMMSCs (0.3×10^6) transfected with Rab27a siRNA or negative control siRNA were loaded in each upper chamber. After three days of co-culture, MRL/*lpr* BMMSCs were used for total RNA isolation, protein isolation and osteogenic differentiation assay.

Supplementary Reference

Akiyama, K., Chen, C., Wang, D., Xu, X., Qu, C., Yamaza, T., Cai, T., Chen, W., Sun, L., and Shi, S. (2012). Mesenchymal-stem-cell-induced immunoregulation involves FAS-ligand-/FAS-mediated T cell apoptosis. Cell Stem Cell *10*, 544-555.

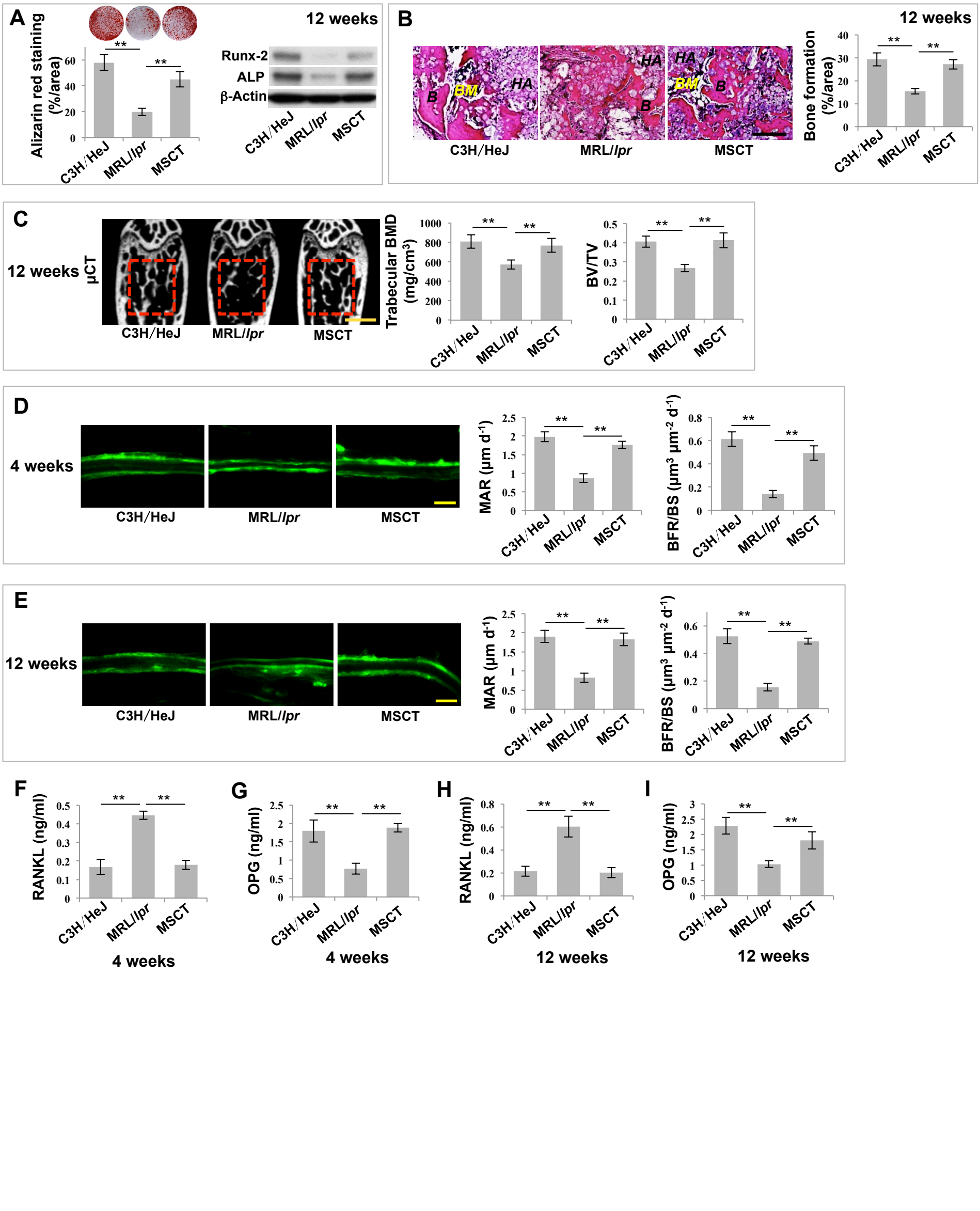
A
12 weeks
Alizarin red staining (%/area)
Runx-2
ALP
β-Actin
C3H/HeJ
MRL/lpr
MSCT
B
12 weeks
BM
HA
B
Bone formation (%/area)
C
12 weeks
μCT
Trabecular BMD (mg/cm³)
BV/TV
D
4 weeks
MAR (μm d⁻¹)
BFR/BS (μm³ μm⁻² d⁻¹)
E
12 weeks
F
RANKL (ng/ml)
4 weeks
G
OPG (ng/ml)
4 weeks
H
RANKL (ng/ml)
12 weeks
I
OPG (ng/ml)
12 weeks

Supplementary Figure 1, related to Figure 1: MSC transplantation (MSCT) rescued impaired BMMSC function and osteoporotic phenotype in MRL/*lpr* mice. (**A**) At 12 weeks post-MSCT, recipient MRL/*lpr* BMMSCs maintained improved mineralized nodule formation capacity, as indicated by Alizarin red staining (n = 5), and expression of osteogenic markers Runx2 and ALP, as assessed by Western blot. (**B**) At 12 weeks post-MSCT, recipient BMMSCs maintained improved *in vivo* new bone formation capacity (n = 5). H&E staining showed newly formed bone (*B*) and bone marrow (*BM*) around HA/TCP (*HA*) carrier when implanted into immunocompromised mice subcutaneously. (**C**) At 12 weeks post-MSCT, MRL/*lpr* mice maintained improved trabecular bone volume, BMD and BV/TV in femurs, as assessed by MicroQCT (n = 5). (**D**) MRL/*lpr* mice showed reduced mineral apposition rate (MAR) and bone formation rate per bone surface (BFR/BS) values compared to wild-type C3H/HeJ mice, as assessed by double calcein labeling of vertebral bodies (LV4). This reduced new bone formation capacity was rescued at 4 weeks post-MSCT (n=5). (**E**) At 12 weeks post-MSCT, MRL/*lp*r mice maintained rescued bone formation capacity, as assessed by MAR and BFR/BS (n=5). (**F, G**) MRL/*lpr* mice showed increased levels of RANKL and decreased levels of OPG in serum when compared to wild-type C3H/HeJ mice. The altered levels of RANKL (**F**) and OPG (**G**) were rescued at 4 weeks post-MSCT, as assessed by ELISA (n = 5). (**H, I**) At 12 weeks post-MSCT, the rescued levels of RANKL (**H**) and OPG (**I**) were maintained, as assessed by ELISA (n = 5). All results are representative of data generated in three independent experiments. Statistical significance was determined with one-way ANOVA. $^{**}P < 0.01$. Error bars: mean ± SD, 200 μm (**B**), 1 mm (**C**), 20 μm (**D, E**).

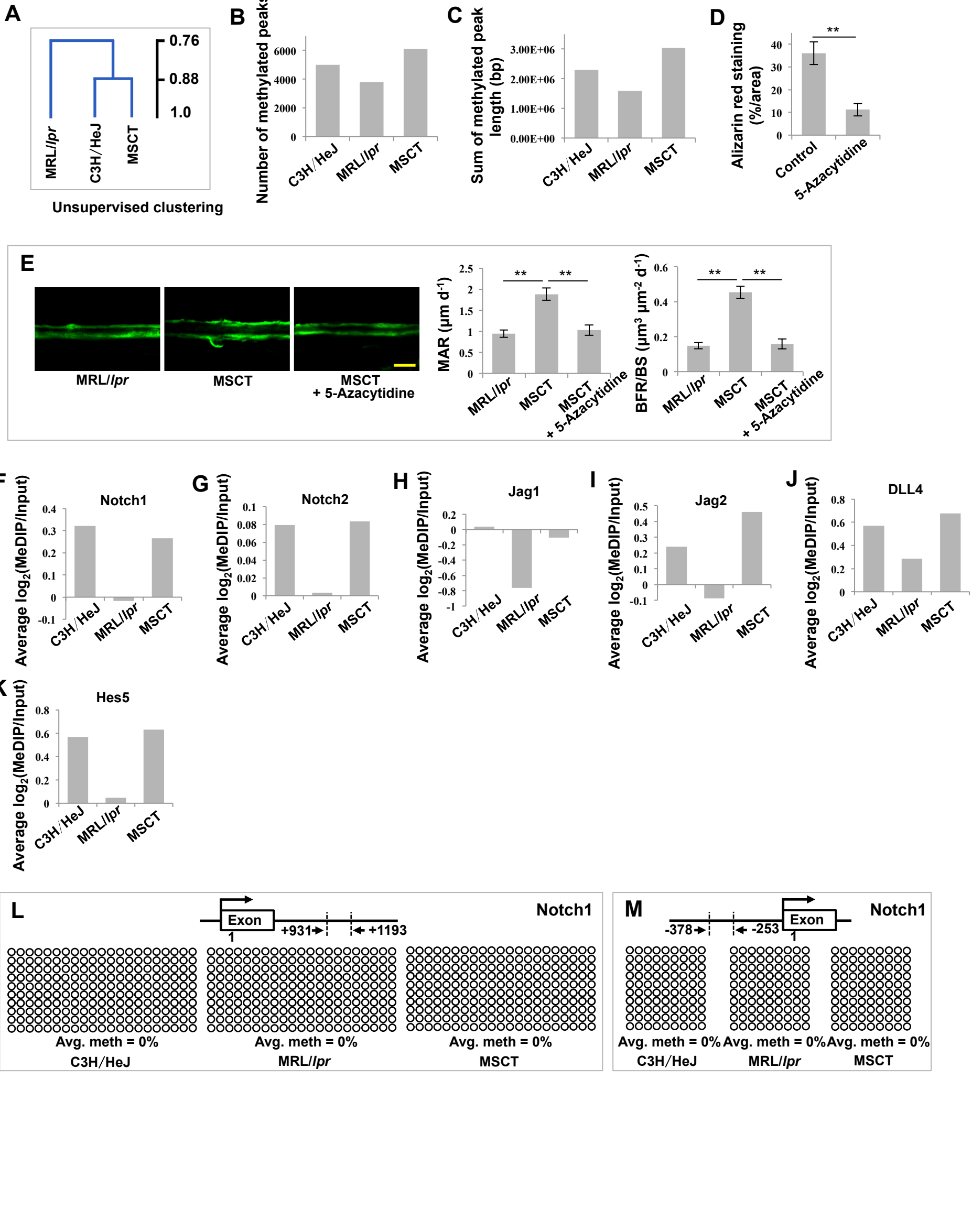
A
0.76
0.88
1.0
MRL/lpr
C3H/HeJ
MSCT
Unsupervised clustering
B
Number of methylated peaks
6000
4000
2000
0
C3H/HeJ
MRL/lpr
MSCT
C
Sum of methylated peak length (bp)
3.00E+06
2.00E+06
1.00E+06
0.00E+00
C3H/HeJ
MRL/lpr
MSCT
D
Alizarin red staining (%/area)
**
40
30
20
10
0
Control
5-Azacytidine
E
MRL/lpr
MSCT
MSCT + 5-Azacytidine
MAR (μm d-1)
**
**
2.5
2
1.5
1
0.5
0
MRL/lpr
MSCT
MSCT + 5-Azacytidine
BFR/BS (μm3 μm-2 d-1)
**
**
0.6
0.4
0.2
0
MRL/lpr
MSCT
MSCT + 5-Azacytidine
F
Notch1
Average log2(MeDIP/Input)
0.4
0.3
0.2
0.1
0
-0.1
C3H/HeJ
MRL/lpr
MSCT
G
Notch2
Average log2(MeDIP/Input)
0.1
0.08
0.06
0.04
0.02
0
C3H/HeJ
MRL/lpr
MSCT
H
Jag1
Average log2(MeDIP/Input)
0.2
0
-0.2
-0.4
-0.6
-0.8
-1
C3H/HeJ
MRL/lpr
MSCT
I
Jag2
Average log2(MeDIP/Input)
0.5
0.4
0.3
0.2
0.1
0
-0.1
C3H/HeJ
MRL/lpr
MSCT
J
DLL4
Average log2(MeDIP/Input)
0.8
0.6
0.4
0.2
0
C3H/HeJ
MRL/lpr
MSCT
K
Hes5
Average log2(MeDIP/Input)
0.8
0.6
0.4
0.2
0
C3H/HeJ
MRL/lpr
MSCT
L
Notch1
Exon
1
+931
+1193
Avg. meth = 0%
C3H/HeJ
Avg. meth = 0%
MRL/lpr
Avg. meth = 0%
MSCT
M
Notch1
-378
-253
Exon
1
Avg. meth = 0%
C3H/HeJ
Avg. meth = 0%
MRL/lpr
Avg. meth = 0%
MSCT

Supplementary Figure 2, related to Figure 1 & Figure 2: MSCT rescued global hypomethylation status of recipient MRL/*lpr* BMMSCs. (**A**) Global methylation status analysis showed that MRL/*lpr* BMMSCs had altered global DNA methylation patterns of gene promoters compared to control C3H/HeJ BMMSCs. MSCT partially rescued altered global methylation patterns of gene promoters in MRL/*lpr* BMMSCs, as assessed by the unsupervised clustering. (**B, C**) Global methylation status analysis showed that MSCT increased the number of methylated peaks (**B**) and sum of methylated peak lengths (**C**) in MRL/*lpr* BMMSC genome. (**D**) 5-Azacytidine treatment (500 nM) inhibited *in vitro* mineralized nodule formation of wild-type C3H/HeJ BMMSCs, as assessed by Alizarin red staining (n = 4). (**E**) 5-Azacytidine treatment (0.5 mg/kg of body weight) blocked MSCT-mediated improvement of new bone formation capacity in MRL/*lpr* mice, as indicated by MAR and BFR/BS (n = 5). (**F-K**) Methylation status of Notch promoters was analyzed using the M value (Average ($\log_2$ MeDIP/Input)). The data showed that the promoters of Notch signaling genes, including Notch1 (**F**), Notch2 (**G**), Jag1 (**H**), Jag2 (**I**), DLL4 (**J**) and Hes5 (**K**) were hypomethylated in MRL/*lpr* BMMSCs. MSCT rescued the hypomethylation status of MRL/*lpr* BMMSCs. (**L, M**) Bisulfite genomic sequencing analysis of the Notch1 promoter regions showed that two regions within exon 1, +931 to +1193 (**L**) and -378 to -253 (**M**), lacked methylated CpGs in BMMSCs derived from wild-type C3H/HeJ mice, MRL/*lpr* mice or MRL/*lpr* mice treated with MSCT. All results are representative of data generated in three independent experiments except DNA methylation microarray analysis. Statistical significance was determined with one-way ANOVA. $^{**}P < 0.01$. Error bars: mean ± SD, 20 μm (**E**).

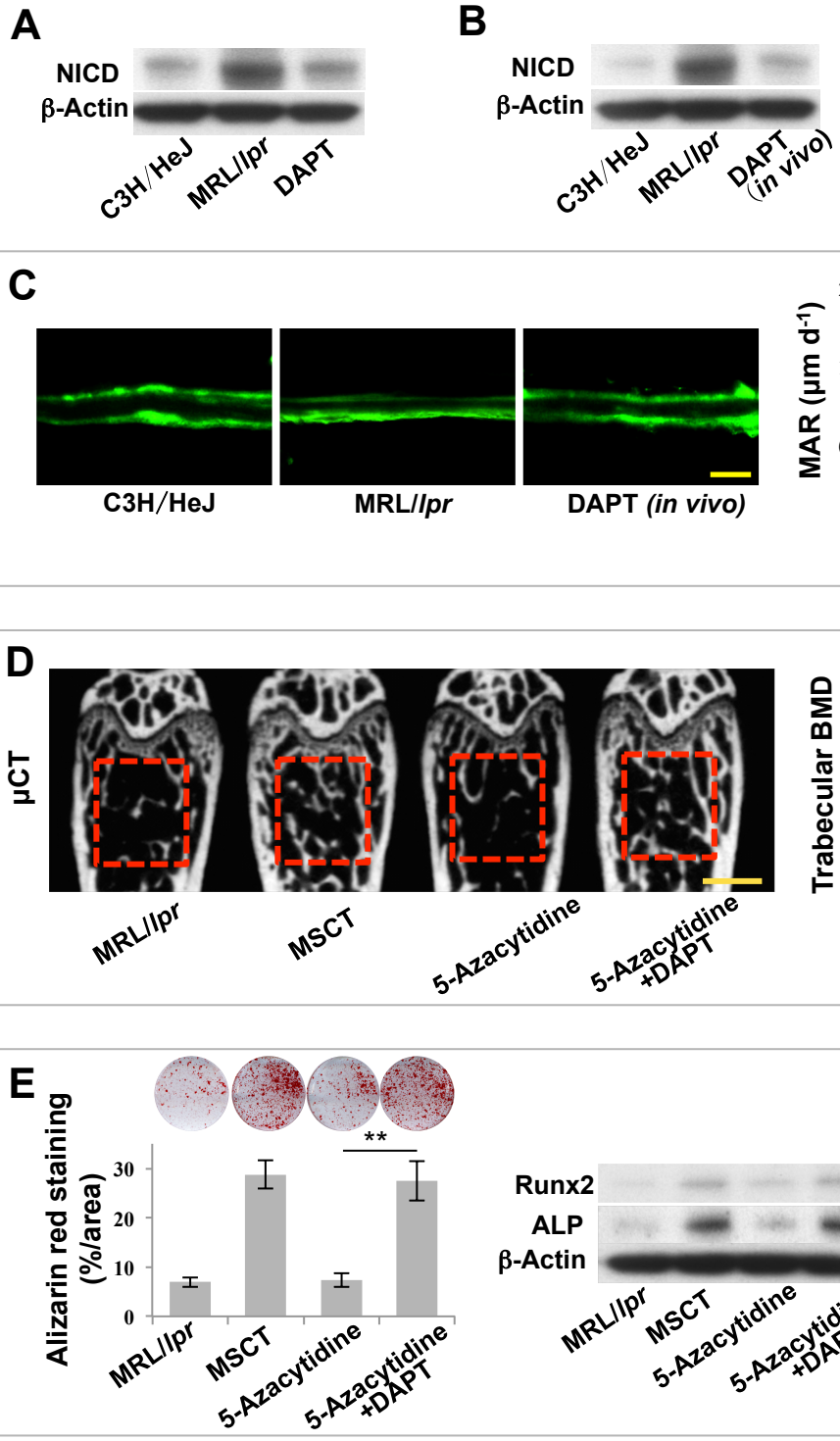
A
NICD
β-Actin
C3H/HeJ
MRL/lpr
DAPT
B
NICD
β-Actin
C3H/HeJ
MRL/lpr
DAPT (in vivo)
C
C3H/HeJ
MRL/lpr
DAPT (in vivo)
MAR (μm d-1)
BFR/BS (μm3 μm-2 d-1)
**
D
μCT
MRL/lpr
MSCT
5-Azacytidine
5-Azacytidine +DAPT
Trabecular BMD (mg/cm3)
BV/TV
E
Alizarin red staining (%/area)
Runx2
ALP
β-Actin
F
Notch1
β-Actin
C3H/HeJ
MRL/lpr
Notch1 siRNA
G
μCT
Trabecular BMD (mg/cm3)
BV/TV
H
Alizarin red staining (%/area)
Runx2
ALP
b-Actin

Supplementary Figure 3, related to Figure 2: MSCT rescued recipient MRL/*lpr* BMMSC function through DNA methylation modification of Notch signaling. (**A**) Western blot analysis showed that *in vitro* DAPT treatment (1 μM) efficiently inhibited NICD expression in MRL/*lpr* BMMSCs. (**B**) Western blot analysis showed that *in vivo* DAPT treatment (10 mg/kg body weight) efficiently inhibited NICD expression in MRL/*lpr* BMMSCs. (**C**) *In vivo* DAPT treatment improved new bone formation in MRL/*lpr* mice, as assessed by MAR and BFR/BS (n = 5). (**D**) *In vivo* DAPT treatments reversed inhibitive effects of 5-Azacytidine on MSCT-mediated rescue of trabecular bone volume, BMD and BV/TV in MRL/*lpr* mice (n=5). (**E**) *In vivo* DAPT treatments reversed inhibitive effects of 5-Azacytidine on MSCT-mediated rescue of mineralized nodule formation capacities of MRL/*lpr* BMMSCs, as indicated by alizarin red staining (n = 5), and expression of osteogenic markers Runx2 and ALP, assessed by Western blot. (**F**) Western blot analysis showed that *in vivo* siRNA knockdown of Notch1 efficiently inhibited Notch1 expression in MRL/*lpr* BMMSCs. (**G**) *In vivo* knockdown of Notch1 partially rescued trabecular bone volume, BMD and BV/TV in MRL/*lpr* mice, as assessed by microQCT (n = 5). (**H**) *In vivo* knockdown of Notch1 partially rescued mineralized nodule formation capacity of MRL/*lpr* BMMSCs, as indicated by alizarin red staining (n = 5), and expression of osteogenic markers Runx2 and ALP, assessed by Western blot. All results are representative of data generated in three independent experiments. Statistical significance was determined with one-way ANOVA. $^{**}P < 0.01$. Error bars: mean ± SD, 20 μm (**C**), 1 mm (**D, G**).

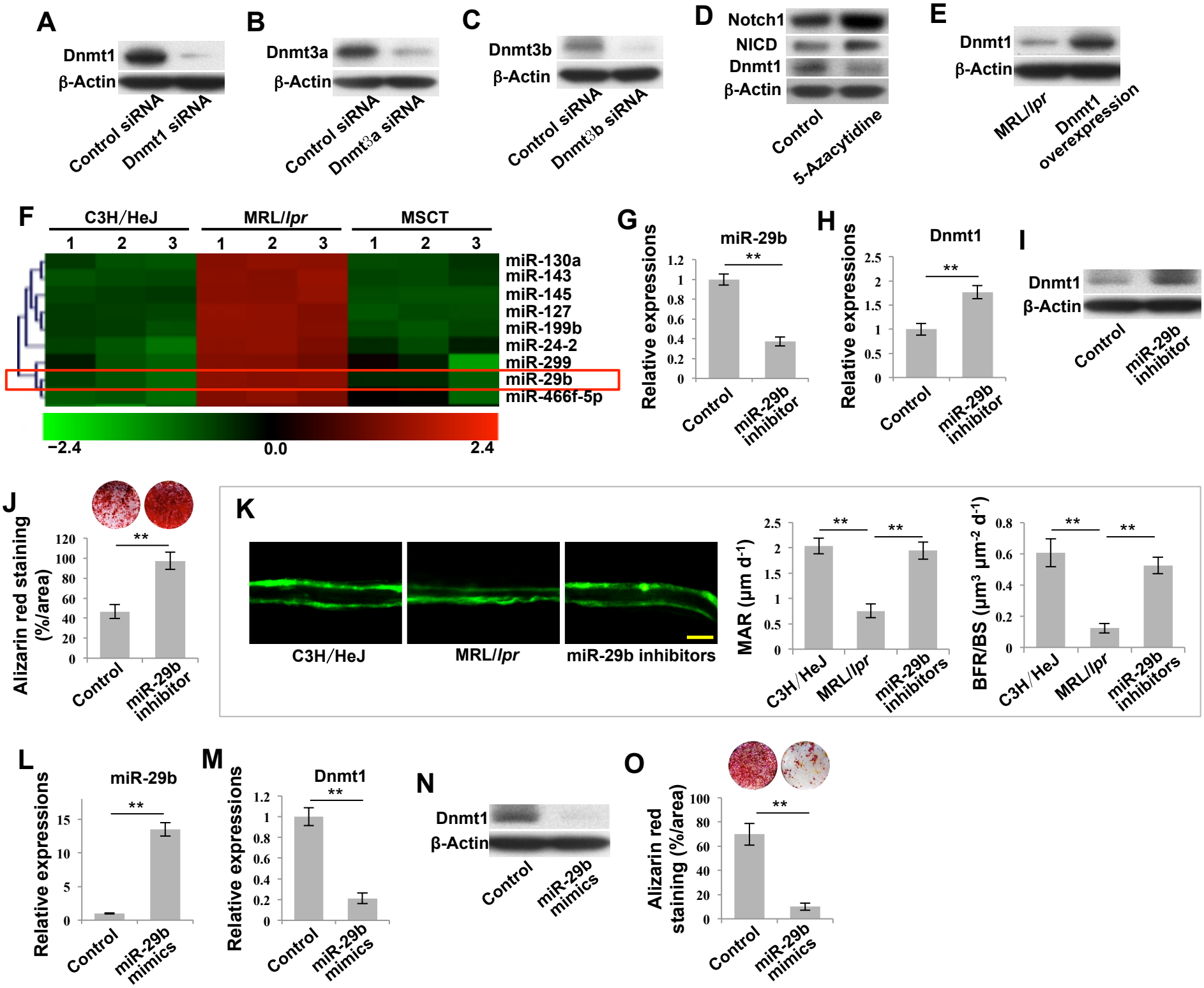

Supplementary Figure 4, related to Figure 3 & Figure 4: miR-29b inhibited Dnmt1 expression in BMMSCs. (**A-C**) Western blot analysis showed that Dnmt1 siRNA (**A**), Dnmt3a siRNA (**B**) and Dnmt3b siRNA (**C**) efficiently inhibited Dnmt1, Dnmt3a, and Dnmt3b expression in BMMSCs. (**D**) 5-Azacytidine treatment promoted the expression of Notch1 and NICD, but inhibited Dnmt1 expression in BMMSCs, as assessed by Western blot. (**E**) Western blot analysis showed that overexpression of Dnmt1 by transfection efficiently increased Dnmt1 expression in MRL/*lpr* BMMSCs. (**F**) miRNA heat map showed that MRL/*lpr* BMMSCs had elevated intracellular levels of miR-29b when compared to control BMMSCs. However, MSCT reduced the levels of miR-29b in MRL/*lpr* BMMSCs. (**G**) Real-time PCR showed that miR-29b inhibitor transfection efficiently inhibited the levels of miR-29b in BMMSCs compared to the negative control group (n = 6). (**H, I**) miR-29b inhibitor treatment promoted the expression of Dnmt1 in BMMSCs, as indicated by real-time PCR (**H**) (n = 6) and Western blot (**I**). (**J**) miR-29b inhibitor treatment elevated mineralized nodule formation, as assessed by alizarin red staining (n = 4). (**K**) *In vivo* miR-29b inhibitor treatment increased new bone formation capacity of MRL/*lpr* mice, as indicated by MAR and BFR/BS (n = 5). (**L**) miR-29b mimic transfection efficiently overexpressed miR-29b in BMMSCs compared to the negative control group (n = 6). (**M, N**) Transfection of miR-29b mimics inhibited Dnmt1 expression in BMMSCs, as indicated by real-time PCR (**M**) (n = 6) and Western blot (**N**). (**O**) Transfection of miR-29b mimics in BMMSCs inhibited mineralized nodule formation, as assessed by alizarin red staining (n = 4). All results are representative of data generated in three independent experiments except miRNA microarray analysis. Statistical significance was determined with Student's t-tests (**G, H, J, L, M, O**) or one-way ANOVA (**K**). $^{**}P < 0.01$. Error bars: mean ± SD, 20 μm (**K**).

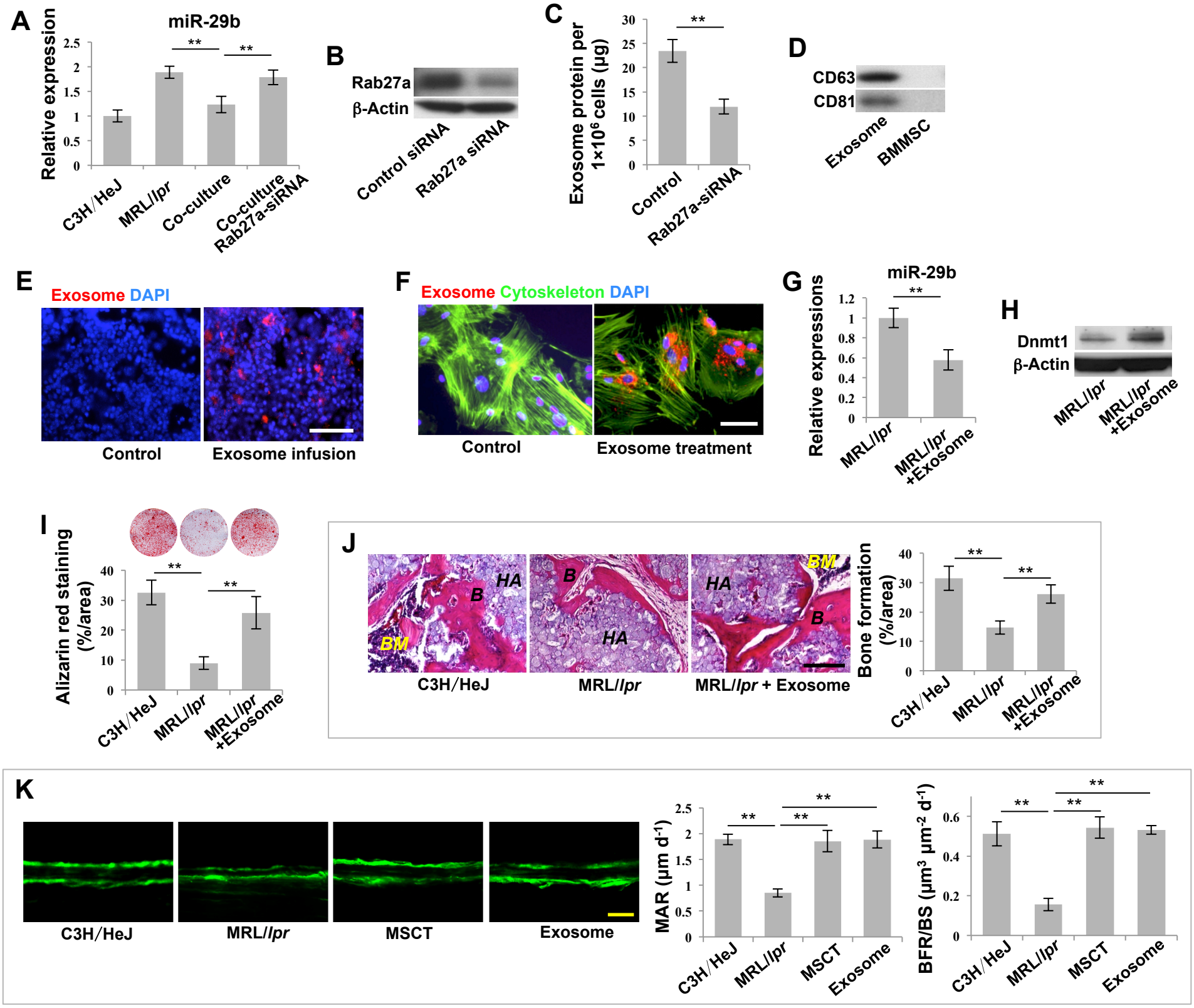

Supplementary Figure 5, related to Figure 5: Exosomes mediated functional recovery of recipient MRL/*lpr* BMMSCs. (**A**) MRL/*lpr* BMMSCs were co-cultured with wild-type BMMSCs using a transwell system. Blockage of exosome release from wild-type BMMSCs by rab27a siRNA knockdown attenuated BMMSC-mediated reduction of intracellular levels of miR-29b (n = 6). (**B**) Western blot analysis showed that Rab27a siRNA efficiently inhibited Rab27a expression in BMMSCs. (**C**) Rab27a siRNA efficiently decreased exosome secretion by BMMSCs, as indicated by total amount of exosome protein purified from culture medium (n = 4). (**D**) Western blot showed that exosomes expressed CD63 and CD81. (**E**) PKH26-labled exosomes were engrossed by bone marrow cells in the MRL/*lpr* mice at 24 hours post-infusion. (**F**) PKH26-labled exosomes were taken in by cultured BMMSCs. (**G-J**) Treatment with exosomes derived from control BMMSCs reduced intracellular levels of miR-29b, assessed by real-time PCR (**G**) (n = 6); elevated expression levels of Dnmt1, assessed by Western blot analysis (**H**); elevated *in vitro* mineralized nodule formation, assessed by alizarin red staining (**I**) (n = 4); and increased *in vivo* new bone formation when implanted into immunocompromised mice subcutaneously (**J**) in MRL/*lpr* BMMSCs (n = 4). (**K**) Systemic infusion of exosomes increased new bone formation capacity of MRL/*lpr* mice, as indicated by MAR and BFR/BS (n = 5). All results are representative of data generated in three independent experiments. Statistical significance was determined with one-way ANOVA (**A, I, J, K**) or Student's t–tests (**C, G**). $^{**}P < 0.01$. Error bars: mean ± SD, 50 μm (**E, F**), 200 μm (**J**), 20 μm (**K**).

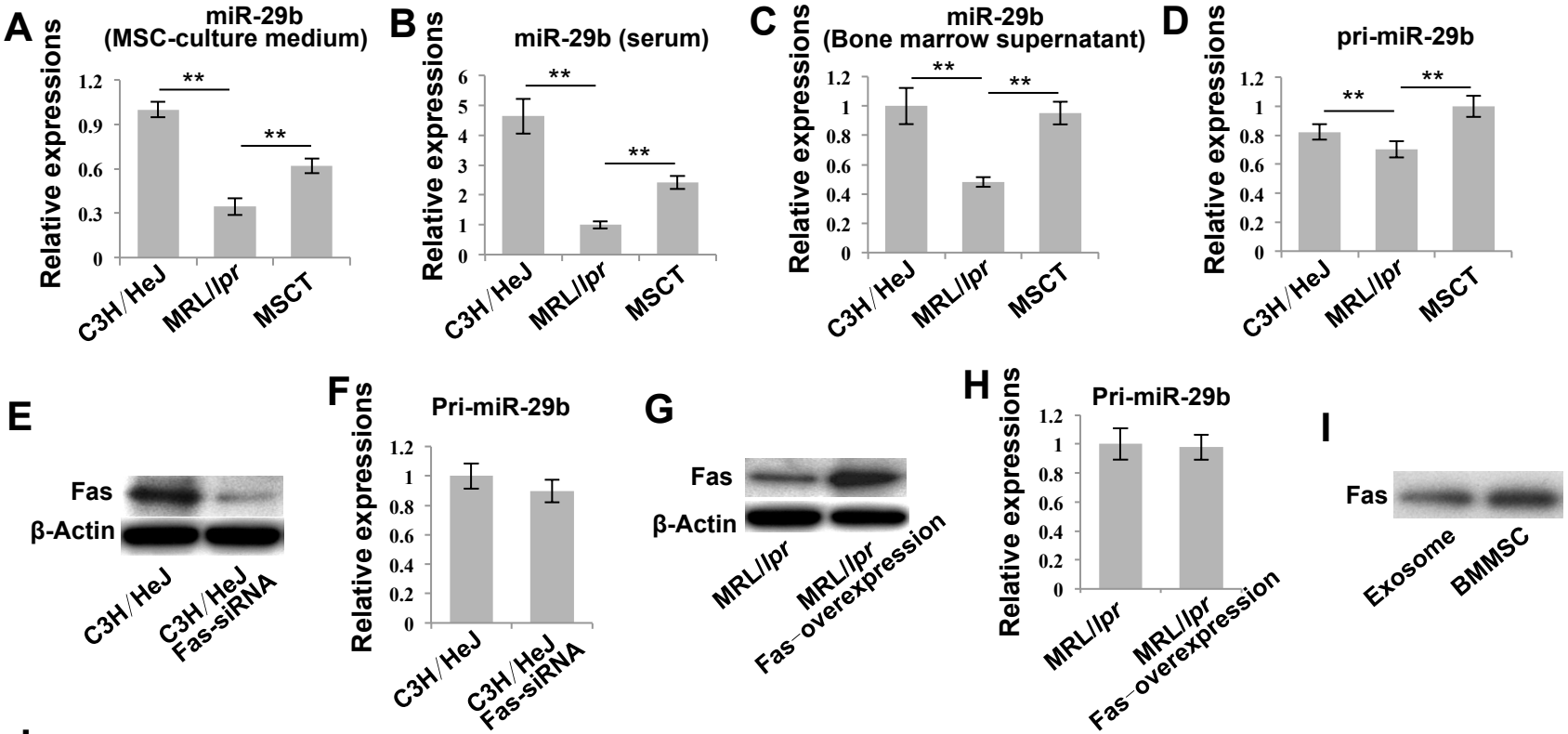

Supplementary Figure 6, related to Figure 6 & Figure 7: Fas governed the levels of intracellular and extracellular miR-29b by controlling miR-29b release. (**A-C**) Real-time PCR analysis showed reduced levels of miR-29b in culture medium of MRL/*lpr* BMMSCs (**A**), MRL/*lpr* mouse serum (**B**) and bone marrow (**C**) when compared to the control groups. MSCT significantly elevated the levels of miR-29b in the culture medium, serum and bone marrow (n = 5). (**D**) Real-time PCR showed that MRL/*lpr* BMMSCs had reduced levels of pri-miR-29b, which was rescued by MSCT (n = 5). (**E**) Western blot analysis showed that Fas siRNA efficiently inhibited Fas expression in BMMSCs. (**F**) Fas knockdown by siRNA failed to significantly affect the pri-miR-29b levels in BMMSCs (n = 6). (**G**) Western blot analysis showed that overexpression of Fas by transfection efficiently increased Fas expression in MRL/*lpr* BMMSCs. (**H**) Overexpression of Fas failed to significantly affect the levels of pri-miR-29b in MRL/*lpr* BMMSCs (n = 6). (**I**) Western blot analysis showed that exosomes contained Fas. BMMSCs were used as a positive control. (**J**) Compared with control empty plasmids, Fas-EGFP fusion protein-expressing plasmid transfection resulted in expression of Fas-EGFP fusion protein in cultured BMMSCs. Immunofluorescent staining showed that BMMSCs co-expressed CD73 with EGFP. All results are representative of data generated in three independent experiments. Statistical significance was determined with one-way ANOVA (**A-D**) or two–tailed Student's t–tests (**F, H**). $^{**}P < 0.01$. Error bars: mean ± SD, 25 μm (**J**).

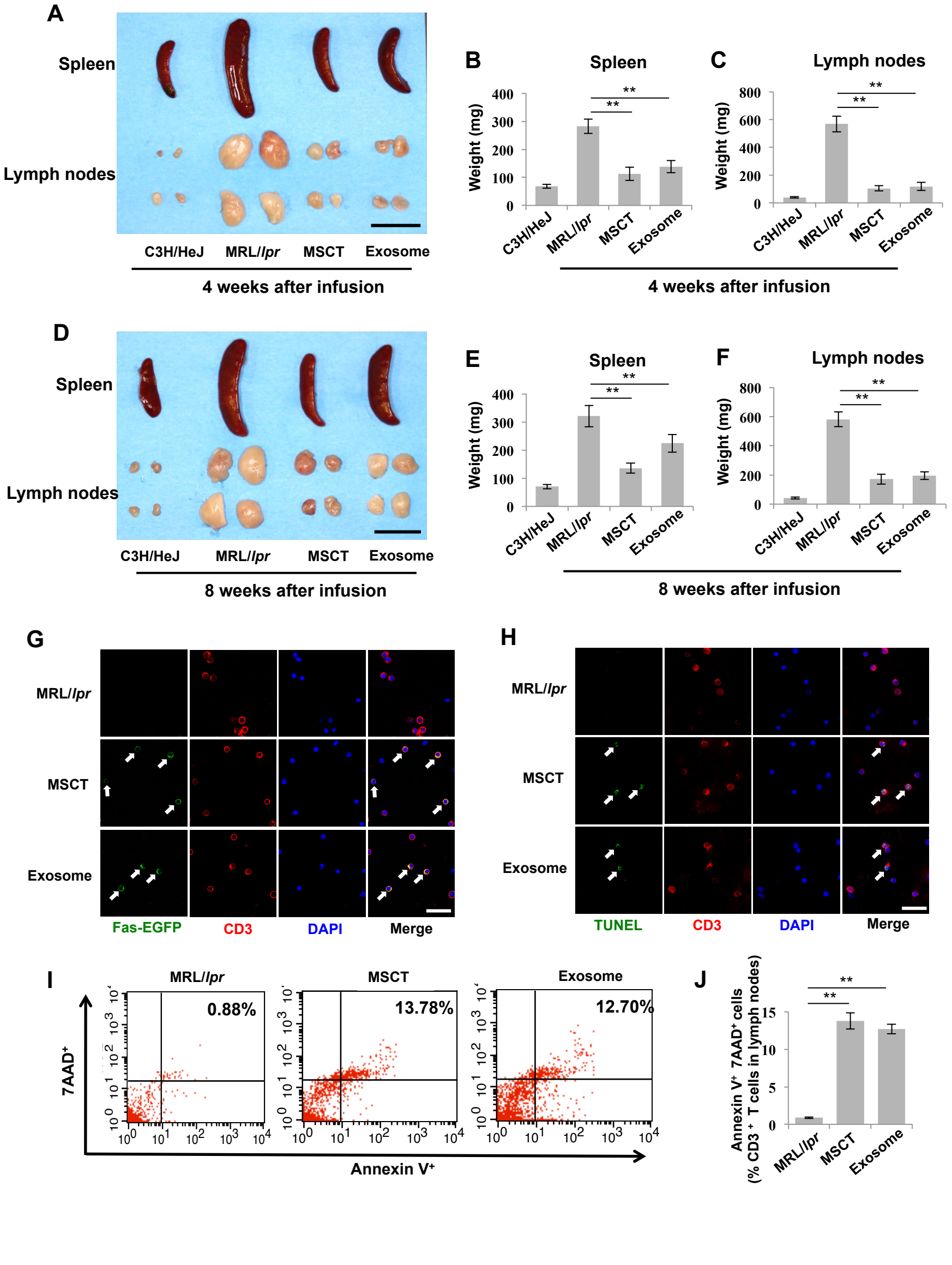
A
Spleen
Lymph nodes
C3H/HeJ
MRL/lpr
MSCT
Exosome
4 weeks after infusion
B
Spleen
Weight (mg)
400
300
200
100
0
**
**
C3H/HeJ
MRL/lpr
MSCT
Exosome
C
Lymph nodes
Weight (mg)
800
600
400
200
0
**
**
C3H/HeJ
MRL/lpr
MSCT
Exosome
4 weeks after infusion
D
Spleen
Lymph nodes
C3H/HeJ
MRL/lpr
MSCT
Exosome
8 weeks after infusion
E
Spleen
Weight (mg)
400
300
200
100
0
**
**
C3H/HeJ
MRL/lpr
MSCT
Exosome
F
Lymph nodes
Weight (mg)
800
600
400
200
0
**
**
C3H/HeJ
MRL/lpr
MSCT
Exosome
8 weeks after infusion
G
MRL/lpr
MSCT
Exosome
Fas-EGFP
CD3
DAPI
Merge
H
MRL/lpr
MSCT
Exosome
TUNEL
CD3
DAPI
Merge
I
MRL/lpr
MSCT
Exosome
0.88%
13.78%
12.70%
7AAD+
Annexin V+
J
Annexin V+ 7AAD+ cells
(% CD3+ T cells in lymph nodes)
15
10
5
0
**
**
MRL/lpr
MSCT
Exosome

Supplementary Figure 7, related to Figure 7: MSCT or exosome infusion reduced spleen and lymph node mass in MRL/*lpr* mice through Fas reuse-mediated T cell apoptosis. (**A-C**) Four weeks after MSCT or exosome (100 μg) infusion, the sizes (**A**) and weights (**B, C**) of spleen and lymph nodes (inguinal, submandibular) in the recipient MRL/*lpr* mice were reduced. (**D-F**) Eight weeks after MSCT or exosome infusion, the sizes (**D**) and weights (**E, F**) of spleen and lymph nodes (inguinal, submandibular) in the recipient MRL/*lpr* mice were reduced. (**G**) BMMSCs (2×10^5) expressing FAS-EGFP or exosomes (100 μg) containing FAS-EGFP were infused into MRL/*lpr* mice. At 24 hours after infusion, FAS-EGFP expressed in $CD3^+$ T cells of lymph nodes was detected by immunofluorescence. (**H**) At 24 hours after BMMSC or exosome infusion, apoptosis of $CD3^+$ T cells of lymph nodes was detected by TUNEL staining combined with immunofluorescence. (**I, J**) The percentage of apoptotic $CD3^+$ T cells was further analyzed by flow cytometry analysis. Statistical significance was determined with one-way ANOVA. $^{**}P < 0.01$. Error bars: mean ± SD, 1 cm (**A, D**), 25 μm (**G, H**).